

THE INERTIAL CAUSE OF WING ROTATION IN DIPTERA

By A. ROLAND ENNOS*

*Department of Biological Sciences, Hatherly Laboratories, University of Exeter,
Prince of Wales Road, Exeter EX4 4PS*

Accepted 5 May 1988

Summary

The cause of the changes in wing pitch at stroke reversal in Diptera has been investigated. The high compliance of the wing base makes it seem unlikely that pitch changes are caused by active torsion at the wing articulation.

The centre of mass of insect wings tends to be behind the centre of torsion of the wing, and it is proposed that wing inertia about the torsional axis alone is responsible for pitch changes as the wing is accelerated at stroke reversal. A simplified inertial model is developed to calculate the angular velocity about the torsional axis that would be caused by wing inertia.

The mass distribution and the torsional axis of the wings of two species of flies was found and it was shown that in these animals inertial causes alone could develop the angular velocity in the pitching plane that is observed at stroke reversal.

Analysis of the movement of individual regions of the wing shows further that inertial effects will produce the tip to base 'torsion wave' seen in the wing at stroke reversal.

Introduction

The kinematics of flight in Diptera has been extensively studied (Nachtigall, 1966, 1981; Vogel, 1966; Weis-Fogh, 1973; Ellington, 1984; Dudley, 1987), and the basic pattern of wing movements is well known. During the two half-strokes the wings are moved through the air along a stroke plane at a more or less constant angle of pitch: about 30–45° from the stroke plane. At the ends of each half-stroke the wings rotate quickly by around 90° to the orientation for the coming stroke. The trailing edge sweeps under the leading edge, until the wing has rotated a few degrees past the pitch angle for the coming stroke, after which it recoils to this position (Ellington, 1984). The wing does not rotate as a flat plate. Anterior and distal areas of the wing rotate first and then a tip to base 'torsion wave' runs along the wing until rotation is complete (Fig. 1).

It has generally been assumed that torque is actively applied by wing base sclerites (Boettiger & Furshpan, 1952; Pfau, 1985; Miyan & Ewing, 1985) which rotate the leading edge of the wing. The torsion is then transmitted quickly along

* Present address: Department of Biological Science, University of York, Heslington, York, YO1 5DD.

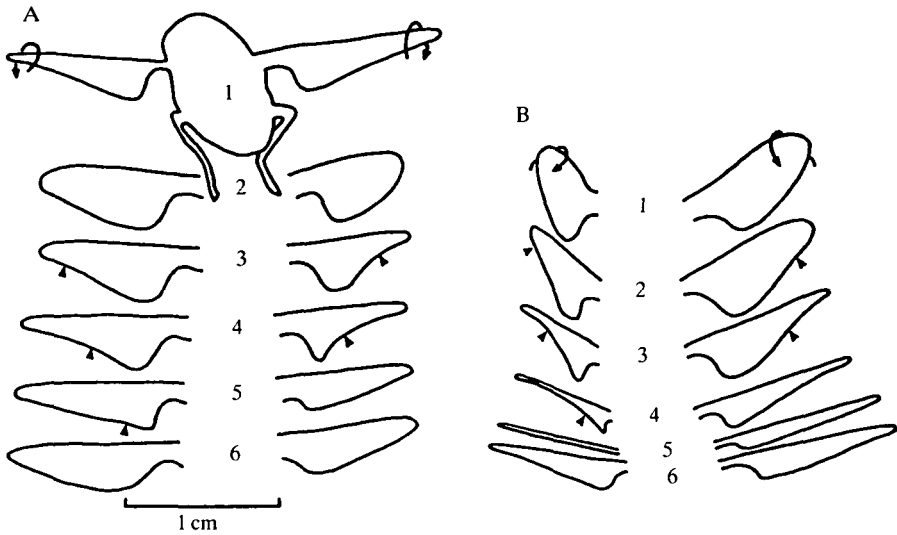


Fig. 1. Film tracings of stroke reversal during the hovering flight of *Eristalis tenax* (insect facing out of page) showing the rotation of the wings. (A) Supination, with the trailing edge sweeping under the leading edge; (B) pronation. The outer regions of the wing rotate first, then a tip to base torsion wave runs in along the wing between frames 3 and 5 in A and 2 and 4 in B. The position of the wave is pointed out by arrowheads. Time between frames, 0.2 ms.

the stiff leading edge to the wing tip, and from there the torsion travels more slowly through the more compliant rear wing region to the base (Wootton, 1981; Ellington, 1984).

I have found, however, that in flies the base of the leading edge is very compliant to torsion (Ennos, 1987, 1988). Torsion applied at the base would not be transmitted immediately to the outer wing. It therefore seems unlikely that control of the wing can be effected in this manner.

In his study on the function of the pterostigma in dragonflies, Norberg (1972) demonstrated the importance of inertial effects on wing rotation. He showed that wing flutter could be caused in gliding flight if the centre of mass of the wing was too far behind its torsional axis, and suggested that wing inertia could control pitch angles at stroke reversals during flapping flight, though neuromuscular control would also operate in many insects.

In this paper I hope to show that no active twisting need be invoked in the case of the Diptera and that the rotational velocity of the wing at stroke reversal and its associated pattern of deformation can both be explained by inertial effects alone.

In a wing flapping with a sinusoidal motion, the torques which cause angular acceleration will be constantly changing. These torques may have several causes. (1) *Inertia*. The centre of mass of an insect wing is often behind its torsional axis (Norberg, 1972). If such a wing is accelerated the inertia of the wing will cause torque to be set up around this axis, and this should rise to a maximum at stroke

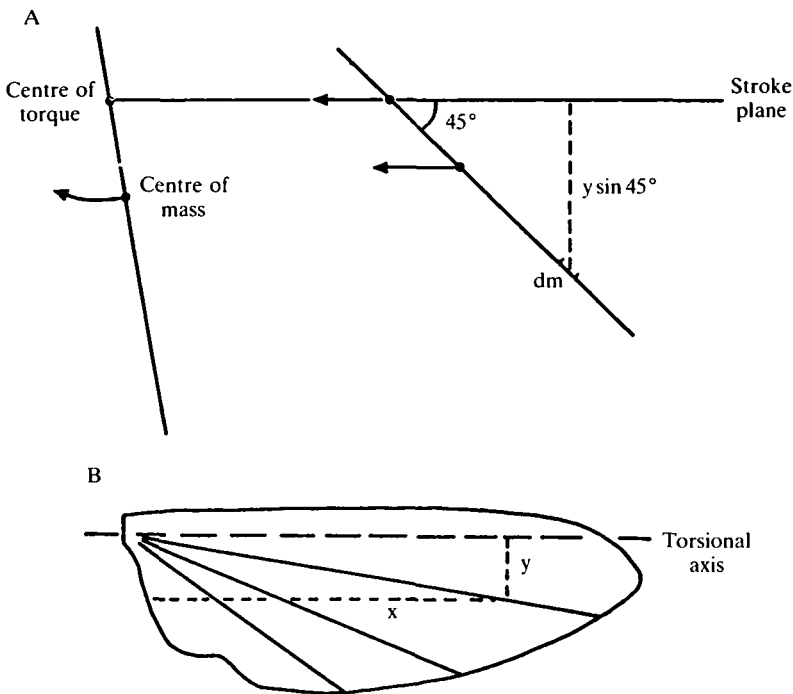


Fig. 2. (A) A wing travelling along a stroke plane with angle of pitch 45° . The centre of mass is behind the torsional axis and so does not move along the same line. The wing possesses angular momentum around the torsional axis which will cause it to rotate when the wing is decelerated. (B) A wing with torsional axis drawn (large dashes). x is the perpendicular distance to a point on the wing from the wing base. y is the perpendicular distance from the torsional axis. Equal values of x/y are shown as lines radiating from the wing base.

reversal, when acceleration is high. (2) *Aerodynamic*. The centre of pressure of aerodynamic forces tends to act behind the torsional axis (Norberg, 1972, 1973; Wootton, 1981). Aerodynamic force will therefore also tend to produce torque, which should rise to a maximum at the middle of each wingbeat, when the wing velocity is greatest. (3) *Elastic recoil*. Elastic recoil of the wing will produce a torque which tends to return it to its rest position. (4) *Active torsion*. The pattern of active torsion is unknown.

A complex differential equation could be built up of the angular wing motion, with estimates of the magnitudes of inertial, aerodynamic and elastic torques and the motion of the wing. The expected rotational velocities could then conceivably be computed numerically. Such an approach, however, as well as being lengthy and possibly inaccurate, does not give an intuitive feel of the problem.

Instead, I have developed a simplified analysis which is based on the principle of conservation of angular momentum. In the middle of a half-stroke there is no rotation in the pitching plane, but the wing has linear momentum which is centred off the torsional axis (Fig. 2A). It thus possesses angular momentum about the

axis. When the wing is decelerated at the end of the beat this angular momentum will remain and cause rotation in the pitching plane. The velocity of rotation is calculated when the torsional axis has been brought to rest and hence in the middle of stroke reversal, halfway through wing rotation. As the wing accelerates into the coming stroke the rotational velocity should become even greater, but further rotation is prevented by mechanical stops on the wing base (Ennos, 1987) and the pitch angle becomes set for the coming half-stroke.

Given knowledge of the mass distribution of the wing and the position of the torsional axis, the resulting angular velocity can be estimated and compared with values from high-speed films.

The analysis

Take a wing in the middle of a half-stroke, travelling along a stroke plane with a positive pitch angle of 45° as is commonly seen (Nachtigall, 1981; Ellington, 1984) (Fig. 2A). The linear momentum dM of a small area of the wing of mass dm , a distance x from the wing base, and a distance y behind the torsional axis (Fig. 2B) will be:

$$dM = x \, dm \, d\phi/dt, \quad (1)$$

where $d\phi/dt$ is the angular velocity of the wing about its base in radians per second. At this positive pitch angle the momentum of this piece of wing is not along the same line as the torsional axis (Fig. 2A). It will therefore possess angular momentum dM_A about the torsional axis, of its linear momentum dM multiplied by its perpendicular distance from the torsional axis, $y\sin 45^\circ$ or about $0.7y$, so:

$$dM_A = 0.7xy \, dm \, d\phi/dt. \quad (2)$$

The angular momentum of the whole wing, M_A is the sum of that of each piece, so:

$$M_A = 0.7d\phi/dt \sum xy \, dm. \quad (3)$$

At mid-stroke the angular velocity of a wing obeying simple harmonic motion (Weis-Fogh, 1973) is $\pi\Phi n$, where Φ is the amplitude of the wingbeat and n is the wingbeat frequency. The total angular momentum, M_A , about the torsional axis will therefore be:

$$M_A = 0.7\pi\Phi n \sum xy \, dm. \quad (4)$$

When the torsional axis of the wing is still, at the end of the half-stroke, this angular momentum remains and should cause rotation of angular velocity ω around the torsional axis:

$$\omega = M_A/I_T, \quad (5)$$

where I_T is the moment of inertia of the wing about the torsional axis:

$$I_T = \sum y^2 dm. \quad (6)$$

Combining equations 4, 5 and 6:

$$\omega = 0.7\pi\Phi n \sum xy \, dm / \sum y^2 \, dm . \quad (7)$$

The average relative velocity, v_r , of the wing edges due to this rotation is the angular velocity multiplied by the mean length of the chord, \bar{c} . This can conveniently be expressed in terms of the length, R , of the wing and the aspect ratio, \mathcal{A} , a measure of the average length/width ratio of a wing pair (Ellington, 1984):

$$\mathcal{A} = 4R^2/S , \quad (8)$$

where S is the combined area of both wings and:

$$\bar{c} = 2R/\mathcal{A} . \quad (9)$$

The average rotational velocity, v_r , is therefore:

$$v_r = 1.4R\pi\Phi n \sum xy \, dm / \mathcal{A} \sum y^2 \, dm . \quad (10)$$

This can be divided by the average velocity of the wing tip, v_t , during wing translation, $2\Phi n R$, to yield a dimensionless ratio of rotational to translational velocities (Ellington, 1984) which can be compared with observed values.

$$v_r/v_t = (0.7\pi/\mathcal{A})(\sum xy \, dm / \sum y^2 \, dm) . \quad (11)$$

If the calculated ratio is less than the observed values then inertia alone is unable to account for the speed of wing rotation.

The virtual mass of the wing is also likely to affect the rotation of the wing. Wing virtual mass, however, is only around a third of the wing mass. If represented by a cylinder of air around the wing, the centre of virtual mass will also be behind the torsional axis of the wing, at the mid-chord. It should therefore produce an effect similar to the wing mass on wing rotation. For these reasons, and also because the actual distribution of the virtual mass is unknown, it is ignored in these calculations.

Materials and methods

Specimens of the hoverfly, *Eristalis tenax*, and the bluebottle, *Calliphora vicina* were killed with ethyl acetate vapour and the torsional axis of a wing was found by pushing it with the point of a mounted needle. The centre of torsion was identified as the line along which a force applied to the wing did not result in either pronation or supination (Norberg, 1972).

The wing was then removed at the base and weighed intact on a Mettler UM3 microbalance, accurate to within $0.1 \mu\text{g}$. It was then placed between two microscope slides and inserted into a photographic enlarger which gave an image magnified by 10 times, and an outline drawing of the wing was made on graph paper. The wing was then cut into rectangular elements 2 mm long and 1 mm broad from the base of the leading edge and each element was weighed. The rest of the wing was kept between the microscope slides to reduce desiccation and conse-

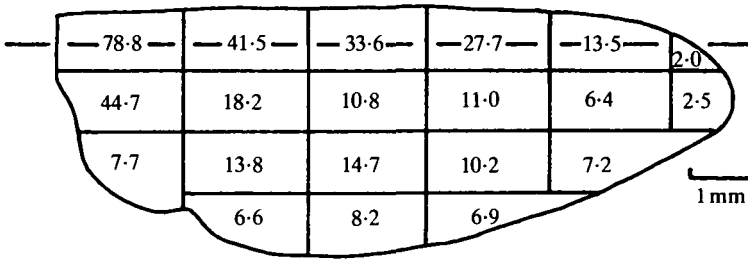


Fig. 3. Mass distribution and torsional axis of the wing of the hoverfly Et.2. Masses are given in micrograms.

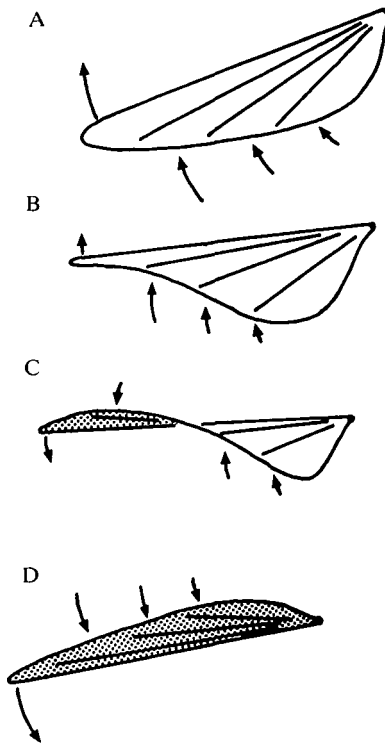


Fig. 4. Tip to base torsion wave at stroke reversal. View from below. As the torsional axis decelerates at the end of the beat (A) anterodistal areas develop a higher angular velocity (shown as longer arrows) and sweep beneath it (B and C) before the inner trailing edge. (D) Reversal complete.

quent weight loss. Typically weight losses were of the order of 10 % of wing mass. Element masses were multiplied by the ratio of wing mass to total strip mass to give corrected figures.

The centre of mass of each element was then estimated from the wing outline, and the wing moment of inertia, y^2dm and the value of $xydm$ about the torsional

Table 1. *Rotational velocity caused by wing inertia*

Insect	R (mm)	\mathcal{AR}	$\sum y^2 dm$ ($\text{kg m}^{-2} \times 10^{-12}$)	$\sum xy dm$	\bar{v}_r/\bar{v}_t
Et.1	12.0	7.6	0.445	1.167	0.76
Et.2	11.2	7.2	0.530	1.158	0.67
Cv.1	8.8	6.3	0.158	0.389	0.86
Cv.2	10.2	5.8	0.364	0.766	0.80
Cv.3	8.7	5.9	0.362	0.637	0.66
Cv.4	9.2	6.0	0.175	0.344	0.72

Results of measurements on hoverflies (Et.1 and 2) and bluebottles (Cv.1-4).

R, wing length; \mathcal{AR} , aspect ratio; \bar{v}_r/\bar{v}_t , calculated ratios of mean rotational to translational velocity.

Explanation of other symbols in text.

Et, *Eristalis tenax*; Cv, *Calliphora vicina*.

axis were calculated. Wing length and area were found using the magnified image and hence the aspect ratio was calculated.

Error in identifying the exact position of the torsional axis was not critical. If the torsional axis was actually further forward than was assumed, the moment arm to the centre of the wing strips would be underestimated, but so would the moment of inertia of the wing. As a result there would be little error in the calculated angular velocity.

Results and discussion

The results of the measurements on individual wings are given in Table 1 and the mass distribution and torsional axis of the wing of the hoverfly Et.2 are shown as an example of the raw data in Fig. 3. In each case the torsional axis of the wing seemed to be along the radial vein, 0.5 mm, or about 15%, of the wing chord behind the leading edge, whereas the centre of wing mass was about 1 mm, or 30% of the wing chord, behind the leading edge. The calculated values for the relative magnitudes of rotational to flapping velocity are also given in the table. Values range from 0.67 to 0.76 in *Eristalis tenax* and from 0.66 to 0.86 in *Calliphora vicina*. Values observed in films range from 0.70 to 0.90 in Ellington's (1984) films of *Eristalis* and 0.58 to 0.79 in my own; values I obtained for *Calliphora* ranged from 0.61 to 1.02. The calculated values fall neatly into the observed range of velocity ratios. Clearly the inertia of the wing is adequate to cause the observed velocities of wing rotation. No active twisting of the wing base need be invoked.

Cause of the torsion wave

A further persuasive feature of this inertial mechanism for pitch change is the ease with which it explains the tip to base torsion wave seen in the insects at stroke

reversal. Take a small area of cuticle a distance x from the wing base and y behind the torsional axis (Fig. 2B). The velocity of the piece at mid-stroke is given by:

$$v = x \, d\phi/dt . \quad (12)$$

During stroke reversal the torsional axis decelerates. If it is not prevented by neighbouring regions, however, the area of wing behind it will keep moving at the same velocity. Its angular velocity around the torsional axis will therefore equal this velocity divided by its distance to the torsional axis, y :

$$\omega = (x/y)d\phi/dt . \quad (13)$$

Therefore the further out along the wing and the closer to the torsional axis is a piece of cuticle (and hence the greater x/y) the faster it will tend to rotate about the torsional axis at stroke reversal. The front and outer part of the wing will rotate most quickly and the basal trailing edge most slowly and the result will be a torsional wave (Fig. 4). The stiffness of the wing will inhibit this to some extent and so those insects with the most flexible rear wing regions (like *Simulium* and *Bibio*) exhibit the torsion wave best, whereas in those insects with relatively stiff wings (like *Drosophila*) the wing rotates more like a flat plate.

Though wing inertia can explain pitch alteration at stroke reversal it is clear that the insects must exert some control, since the timing of wing rotation can be altered in flight (Ellington, 1984).

I thank Dr R. J. Wootton for his help and criticism during the work and in the production of the manuscript. The work was carried out while under tenure of an SERC research studentship.

References

- BOETTIGER, E. G. & FURSHPAN, E. (1952). The mechanics of flight movements in Diptera. *Biol. Bull. mar. biol. Lab., Woods Hole* **102**, 200–211.
- DUDLEY, T. R. (1987). The mechanics of forward flight in insects. Ph.D. thesis, University of Cambridge.
- ELLINGTON, C. P. (1984). The aerodynamics of hovering insect flight. III. Kinematics. *Phil. Trans. R. Soc. Ser. B* **305**, 41–78.
- ENNOS, A. R. (1987). A comparative study of the flight mechanism of Diptera. *J. exp. Biol.* **127**, 355–372.
- ENNOS, A. R. (1988). The importance of torsion in the design of insect wings. *J. exp. Biol.* **140**, 137–160.
- MIYAN, J. A. & EWING, A. W. (1985). How Diptera move their wings: a re-examination of the wing base articulation and muscle systems concerned with flight. *Phil. Trans. R. Soc. Ser. B* **311**, 271–302.
- NACHTIGALL, W. (1966). Die Kinematik der Schlagflügelbewegungen von Dipteren. Methodische und Analytische Grundlagen zur Biophysik des Insektenflugs. *Z. vergl. Physiol.* **52**, 155–211.
- NACHTIGALL, W. (1981). Insect flight aerodynamics. In *Locomotion and Energetics in Arthropods* (ed C. F. Herreid & C. R. Fourtner), pp. 127–162. New York: Plenum Press.
- NORBERG, R. Å. (1972). The pterostigma of insect wings an inertial regulator of wing pitch. *J. comp. Physiol.* **81**, 9–22.
- NORBERG, R. Å. (1973). Autorotation, self-stability, and structure of single-winged fruits and seeds (samaras) with comparative remarks on animal flight. *Biol. Rev.* **48**, 561–596.

- PFAU, H. K. (1985). Zur funktionellen und phylogenetischen Bedeutung der "Gangschaltung" der Fliegen. *Verh. dt. zool. Ges.* **78**, 168.
- VOGEL, S. (1966). Flight in *Drosophila*. I. Flight performance of tethered flies. *J. exp. Biol.* **44**, 567–578.
- WEIS-FOGH, T. (1973). Quick estimates of flight fitness in hovering animals, including novel mechanisms for lift production. *J. exp. Biol.* **59**, 169–230.
- WOOTTON, R. J. (1981). Support and deformability in insect wings. *J. Zool., Lond.* **193**, 447–468.

